Quaternary Research 82 (2014) 450–461

Contents lists available at ScienceDirect

Quaternary Research

journal homepage: www.elsevier.com/locate/yqres

A continuous stable isotope record from the penultimate glacial maximum to the Last Interglacial (159–121 ka) from Tana Che Urla Cave (Apuan Alps, central Italy)

Eleonora Regattieri [a,b,*], Giovanni Zanchetta [a,b,c], Russell N. Drysdale [d], Ilaria Isola [c], John C. Hellstrom [e], Adriano Roncioni [f]

[a] Dipartimento di Scienze della Terra, Via S. Maria 53 56126 Pisa, Italy
[b] Istituto di Geoscienze e Georisorse IGG-CNR, via Moruzzi 1, 56100 Pisa, Italy
[c] Istituto Nazionale di Geofisica e Vulcanologia INGV, Via della Faggiola 32, Pisa, Italy
[d] Department of Resource Management and Geography, University of Melbourne, Victoria 3010, Australia
[e] School of Earth Sciences, University of Melbourne, Victoria 3010 Australia
[f] Gruppo Speleologico Lucchese, via Don Minzoni, Lucca, Italy

ARTICLE INFO

Article history:
Received 23 January 2014
Available online 28 June 2014

Keywords:
Speleothem
Stable isotopes
Central Italy
Penultimate deglaciation
Last Interglacial

ABSTRACT

Relatively few radiometrically dated records are available for the central Mediterranean spanning the marine oxygen isotope stage 6–5 (MIS 6–5) transition and the first part of the Last Interglacial. Two flowstone cores from Tana che Urla Cave (TCU, central Italy), constrained by 19 U/Th ages, preserve an interval of continuous speleothem deposition between ca. 159 and 121 ka. A multiproxy record ($\delta^{18}O$, $\delta^{13}C$, growth rate and petrographic changes) obtained from this flowstone preserves significant regional-scale hydrological changes through the glacial/interglacial transition and multi-centennial variability (interpreted as alternations between wetter and drier periods) within both glacial and interglacial stages. The glacial stage shows a wetter period between ca. 154 and 152 ka, while the early to middle Last Interglacial period shows several drying events at ca. 129, 126 and 122 ka, which can be placed in the wider context of climatic instability emerging from North Atlantic marine and NW European terrestrial records. The TCU record also provides important insights into the evolution of local environmental conditions (i.e. soil development) in response to regional and global-scale climate events.

Introduction

The timing and climatic evolution of the penultimate deglaciation (Termination II in the deep-sea sediment record) and the succeeding interglacial (marine oxygen isotope stage (MIS) 5e) are relevant to understanding both the mechanisms of ice-age cycles in general and, more specifically, the background of natural climate variability during interglacials and how the present interglacial may come to an end (e.g. Kukla et al., 1997, 2002; Broecker and Henderson, 1998; Tzedakis et al., 2009). In particular, there is increasing evidence that the climate of the Last Interglacial was unstable relative to the Holocene. This variability was first identified in North Atlantic marine sediments (e.g. McManus et al., 1994; Bond et al., 2001; Oppo et al., 2001; Heusser and Oppo, 2003) and, at least for the most prominent events, this instability propagated into southern Europe and the Mediterranean basin (e.g. Martrat et al., 2004; Sanchez-Goni, 2005; Sprovieri et al., 2006; Brauer et al., 2007; Couchoud et al., 2009). This instability has been related to hydrographic changes in the dynamics of the North Atlantic Meridional Overturning Circulation (MOC). However, the timing and geographical persistence of MIS 5e variability are still relatively poorly known, with many of the climatic oscillations yet to be identified and their impacts still poorly understood beyond the North Atlantic region. In particular, independently (e.g. radiometrically) dated records of the penultimate deglaciation and Last Interglacial in the Mediterranean basin are rare (e.g. Bar-Matthews et al., 2000; Drysdale et al., 2005, 2009; Vogel et al., 2009; Lezine et al., 2010) and, in this context, the most chronologically robust archives for paleoclimate reconstruction on land have been speleothems because of their well-demonstrated high sensitivity to climate changes and their capability to be dated precisely by U/Th methods (e.g. Bar-Matthews et al., 1999; Richards and Dorale, 2003).

In this study we present petrographic, growth-rate and stable-isotope data from two flowstone cores collected from Tana che Urla Cave (TCU, Apuan Alps NW Tuscany, central Italy, Fig. 1), which show continuous growth between ca. 159 and 121 ka. The aim of this work

* Corresponding author at: Dipartimento di Scienze della Terra, Via S. Maria 53 56126 Pisa, Italy.
E-mail address: regattieri@dst.unipi.it (E. Regattieri).

http://dx.doi.org/10.1016/j.yqres.2014.05.005
0033-5894/

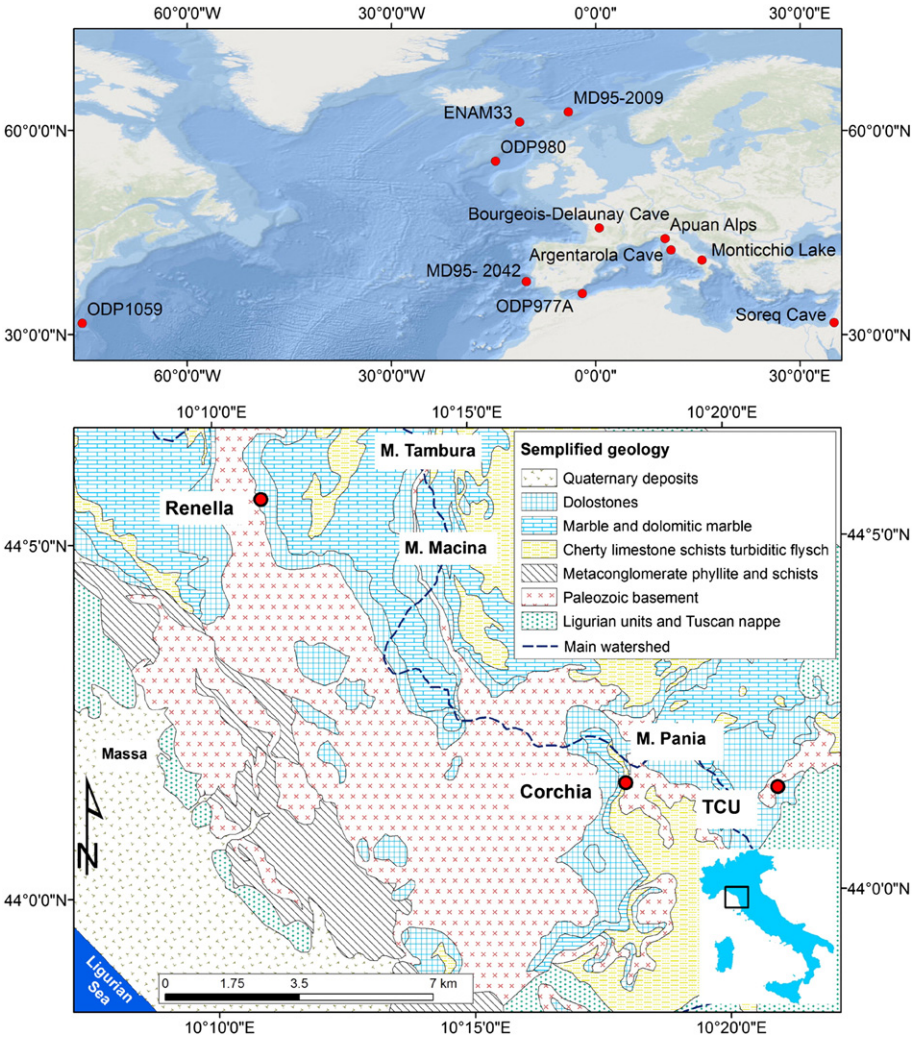

Figure 1. Top: location of the Apuan Alps and other sites mentioned in the text; Bottom: simplified geology of the Apuan Alps showing mean peaks and locations of Tana che Urla, Corchia and Renella Caves.

is to investigate the regional hydrological changes occurring at the glacial/interglacial transition and to investigate the presence of centennial-scale variability during both the penultimate glacial and the first part of the Last Interglacial.

Cave setting

Tana che Urla (TCU) (Fig. 1) is a sub-horizontal spring cave (592 m total length, of which 370 m is emerged and 222 m is submerged; 45 m total height difference) that opens at 620 m asl on the south-eastern side of the Pania massif, in the Apuan Alps (NW Tuscany, central Italy). The cave has developed at the contact between metasiliclastics and schists (Fornovolasco schist formation), and Triassic meta-dolomite (known as the Grezzoni formation Pandeli et al., 2004). Inside the cave there is a permanent stream, which represents the terminal part of an underground collector system that drains the southern slope of Pania della Croce Mountain (1858 m asl).

The valley above the cave is covered by forest, mainly of cultivated chestnuts (*Castanea sativa*) at lower altitude, and beech (*Fagus sylvatica*) at higher altitude; the summit part (above ca. 1600 m asl) hosts a grassland dominated by the genus *Brachipodium*. All plants belong to the C3-type vegetation category.

The local climate is wet throughout the year, with a mean annual precipitation of about 2500 mm/yr recorded at the nearby village of Fornovolasco (data spanning 1951 to 1995: Piccini et al., 1999) but higher (more than 3000 mm/yr) on the ridge of Pania della Croce. Such high precipitation is due to the strong Apuan Alps orographic effect, which traps eastward-moving moisture. Analyses of air-mass back trajectories show that the western Mediterranean and North Atlantic are the dominant sources of local rainfall (Drysdale et al., 2004). There is no official temperature record nearby, but the mean annual temperature (MAT) of the site recorded inside the cave (discontinuously monitored since 2008; $n = 7$) is 10.2°C (SD 0.5°C).

Irregular samples of drip waters collected in recent years show a near-constant oxygen isotope composition (-7.13 ± 0.27‰, $n = 7$). Based on previous work by Mussi et al. (1998), these values are consistent with a local recharge area at ca. 800–700 m asl and a rain-shadow effect on the isotopic composition of meteoric precipitation exerted by Apennine divide.

Materials and methods

Two cores, TCU-D3 and TCU-D4 (Fig. 2, herein referred to as D3 and D4), were drilled about 1.5 m from one another, from the same flowstone mass located in the main branch of the cave. Core D3 was drilled from a lower-angle, lower lobe of the flowstone, whereas D4 was extracted from a lobe in a steeper part of the flowstone. The sample location is ca. 100 m from the cave entrance, on the left bank of the cave stream, ca. 3 m above the current river level. D4 and D3 are 350 mm and 640 mm long respectively. In both cores the bedrock was reached.

https://doi.org/10.1016/j.yqres.2014.05.005 Published online by Cambridge University Press

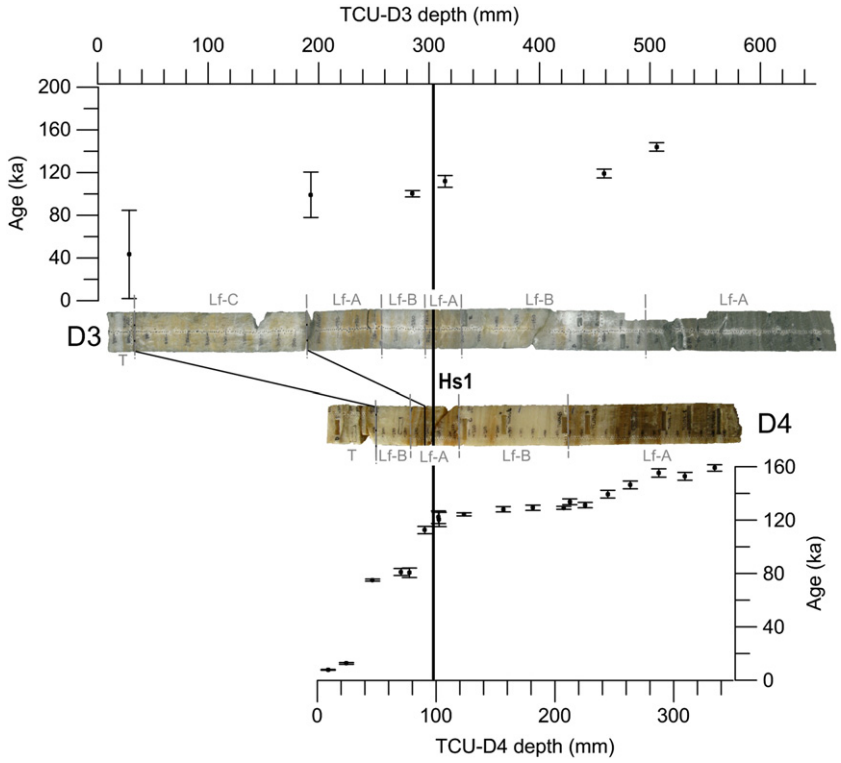

Figure 2. Middle: TCU cores D3 (top) and D3 (bottom), showing stratigraphic correlations and main lithofacies (in grey) from Regattieri et al. (2012). Top (D3) and bottom (D4): ages vs. depth (mm from top). 'Hs1' is the hiatus, which marks the end of the discussed section — see main text for details.

Polished sections of each core were sub-sampled for stable C and O isotope ($\delta^{18}O$ and $\delta^{13}C$) analyses perpendicular to the growth laminations. D4 was sampled at 1 mm increments using a milling machine with a 1 mm-diameter drilling bit, producing 350 samples. D3 was sampled with a manual drill (1 mm-diameter drilling bit) at ca. 1.5–2.0 mm increments, producing 393 samples. $\delta^{18}O$ and $\delta^{13}C$ isotope ratios were measured using a GV2003 continuous-flow isotope ratio mass spectrometer at the University of Newcastle, Australia. All results are reported relative to the Vienna Pee Dee Belemnite (V-PDB) international scale. Sample results were normalised to this scale using a Carrara Marble standard (NEW1) previously calibrated using the international standards NBS-18 and NBS-19. Analytical uncertainty for $\delta^{18}O$ and $\delta^{13}C$ was 0.09 ‰ and 0.05‰ respectively.

Nineteen samples from both cores were taken for U/Th dating. Owing to the likelihood of large uncertainties in the results due to clastic contamination and low uranium content in the flowstone, solid prisms of ca. 200 mg (ca. 3 mm wide along the lamina and 1 mm thick on growth axis) were used. The U/Th dating was performed at the University of Melbourne (Victoria, Australia) following the method of Hellstrom (2003). Briefly, samples were dissolved and a mixed ^{236}U-^{233}U-^{229}Th spike was added prior to removal of the carbonate matrix with ion-exchange resin. The purified U and Th fraction was introduced in a dilute nitric acid to a multi-collector inductively coupled plasma mass spectrometer (MC-ICPMS, Nu-Instruments Plasma). The $^{230}Th/^{238}U$ and $^{234}U/^{238}U$ activity ratios were calculated from the measured atomic ratios using an internally standardised parallel ion-counter procedure and calibrated against the HU-1 secular equilibrium standard. Correction for detrital Th content was applied using initial activity ratios of detrital thorium $(^{230}Th/^{232}Th)_i$ of 2.55 ± 0.80 and 2.95 ± 0.45 for D4 and D3 respectively. These values and their relative 2σ uncertainty were calculated using a Monte Carlo 'stratigraphic constraint' procedure based on the series of U/Th ages from both cores (Hellstrom, 2006). Under this method, the $(^{230}Th/^{232}Th)_i$ and its uncertainty are optimized in order to bring all ages into correct stratigraphic order (i.e. with the assumption that age must increase with depth from top) within their age uncertainties. A depth–age model (Fig. 3) for core D4 was constructed using a Bayesian Monte Carlo approach (Drysdale et al., 2005; Scholz et al., 2012).

Results

The chronology of D4 is better constrained compared to D3, which seems to be more affected by clastic contamination (Table 1), perhaps because the flowstone lobe from which D3 was taken is inclined at a lower angle than the D4 site, facilitating a greater build up and incorporation of detrital particles during calcite deposition. Consequently, after preliminary dating, the process of improving the age model was achieved by a greater focus on core D4. Age constraints indicate that D4 shows continuous growth between ca. 158.5 ± 2.7 and 121.4 ± 3.0 ka and henceforth will be considered as the 'master core'. Herein, we focus mostly on the basal section (237 mm) of D4. The upper section

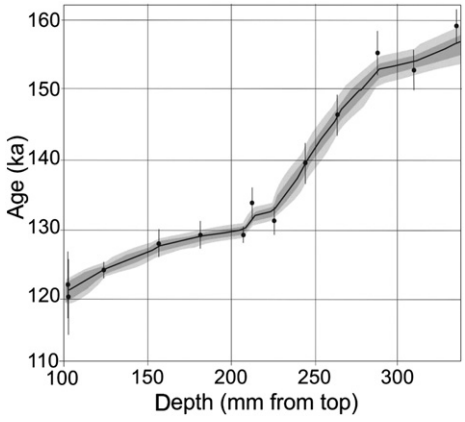

Figure 3. Depth–age model (depth from core top in mm) for the discussed section of continuous growth of core D4. The outer shaded zones define the 95% uncertainties.

https://doi.org/10.1016/j.yqres.2014.05.005 Published online by Cambridge University Press

Table 1
Corrected U/Th ages for TCU D3 and TCU D4 cores. The activity ratios have been standardized to the HU-1 secular equilibrium standard, and ages calculated using decay constants of 9.195×10^{-6} (^{230}Th) and 2.835×10^{-6} (^{234}U). Depths are from top, whilst the numbers in brackets are the 95% uncertainties.

Sample ID	^{238}U ng/g	Depth/mm	(^{230}Th/^{238}U)	(^{234}U/^{238}U)	(^{232}Th/^{238}U)*1000	^{230}Th/^{232}Th	Age, ka	2 s.e.
TCUD4-D	30	9.1	0.10	1.35	3.91	26.18	7.79	(0.28)
TCUD4-24.5	25	24.5	0.17	1.33	9.75	17.15	12.61	(0.65)
TCUD4-46.5	29	46.5	0.66	1.28	5.91	111.43	75.03	(0.78)
TCUD4-70.5	25	70.5	0.72	1.27	31.77	22.59	81.12	(2.61)
TCUD4-77.5	25	77.5	0.72	1.24	48.35	14.86	80.52	(3.56)
TCUD4-90.5	18	90.5	0.84	1.24	30.71	27.48	112.55	(2.77)
TCUD4-102.5A	21	102.5	0.91	1.24	70.09	12.97	120.44	(5.36)
TCUD4-102.5B	18	102	0.91	1.24	62.34	14.57	122.15	(4.68)
TCUD4-C	42	123.5	0.81	1.16	6.19	131.25	124.30	(1.16)
TCUD4-4	52	156.5	0.87	1.22	5.96	146.66	128.10	(1.98)
TCUD4-181.5	41	181.5	0.88	1.22	5.60	156.71	129.24	(1.98)
TCUD4-B	64	207.5	0.88	1.23	7.11	124.47	129.21	(1.10)
TCUD4-212.5	34	212.5	0.90	1.23	6.82	132.55	133.73	(2.17)
TCUD4-3	50	225.5	0.91	1.24	17.07	53.15	131.23	(2.01)
TCUD4-244.5	43	244.5	0.93	1.23	30.38	30.73	139.44	(2.89)
TCUD4-263.5	43	263.5	0.95	1.22	27.60	34.37	146.38	(2.91)
TCUD4-2	71	287.5	0.95	1.20	22.75	41.79	155.30	(3.12)
TCUD4-1	52	309.5	0.95	1.20	18.67	50.65	152.83	(2.94)
TCUD4-A	54	334.5	0.94	1.18	6.01	155.79	159.08	(1.3)
TCU D3 A_d	27	28.5	0.67	1.28	0.23	0.23	43.37	(41.35)
TCU D3 Abis C	42	190.0	1.06	1.26	0.25	0.25	99.26	(21.38)
TCU D3 Abis.b	35	281.0	0.76	1.22	0.01	0.01	100.25	(2.97)
TCU D3 E	36	313.0	0.89	1.19	0.10	0.10	111.826	(5.50)
TCU D3 C	89	458.5	0.91	1.21	0.08	0.08	119.164	(4.16)
TCU.D3 B_e	74	509.5	0.98	1.22	0.07	0.07	144.10	(3.98)

of both cores display several growth interruptions and their age profiles are poorly constrained, warranting only brief discussion.

Stratigraphy

Both cores (Fig. 2) are mainly composed of columnar calcite, which ranges from poorly-to-well laminated to massive, often with a persistent detrital component. Based on the clastic content, fabrics, visual appearance and color of the calcite, Regattieri et al. (2012) defined two main lithofacies (Fig. 4). Lithofacies (Lf) A is richest in clastic material and is characterised by grey–brown calcite with thin laminations of sediment, while Lf-B is composed of compact, milky calcite, with little to no evidence of lamination and a lower content of impurities. Following Regattieri et al. (2012), the discussed sections of D4 and D3 show a basal portion of Lf-A that spans from the start of the deposition at ca. 159 ka to ca. 132 ka (depth 348–208 mm on D4 and 639–439 mm on D3; ages from the D4 age model), followed by Lf-B until the first growth interruption (Hiatus Hs1) at ca. 121 ka (depth 95 mm on D4, 299 mm on D3). This hiatus is clearly recognizable in both cores (Hs1 in Figs. 2 and 4) and marks the end of the interval discussed here. The upper part of both cores shows further alternation between the two defined lithofacies, although the sequence is thicker in core D3, and also contains another type of calcite that is more porous and contains microgour remnants (Lf-C of Regattieri et al., 2012).

Chronology

TCU speleothems are characterised by a low uranium content (average concentration in both cores is 42 ppb, minimum = 18 ppb, maximum = 89 ppb; see Table 1) and persistent detrital contamination (i.e. low ^{230}Th/^{232}Th, see Table 1), which is particularly pronounced in the Lf-A lithofacies (Regattieri et al., 2012). The 13 corrected ^{230}Th ages of the lower section of core D4 range from 159.1 ± 1.3 ka before present to 120.4 ± 5.4 ka (Fig. 2 and Table 1). Six ages from the upper section of D4, above the Hs1 hiatus, indicate brief intervals of late MIS 5, Late Glacial and Holocene growth (Fig. 2).

Four of the six corrected ^{230}Th ages on core D3 range from 144.1 ± 4.0 ka to 100.3 ± 3.0 ka, and are in stratigraphic order. Three of these are contained in the lower section (before hiatus Hs1; Fig. 2, Table 1) and one just above the hiatus. Two further ages from this core (Table 1, Fig. 2) are reported only for completeness but, due to their large errors, they do not add useful information to this study. Hiatus Hs1, which marks the end of the discussed interval, is constrained in core D4 to between ca. 120.4 ± 2.0 and 112.5 ± 2.8 ka.

The upper section of the TCU flowstone shows discontinuous growth for late MIS 5, with deposition at ca. 112.6 ± 2.8 ka in core D4 and at 100.3 ± 3 ka in core D3. Stratigraphic correlation between the two cores (Regattieri et al., 2012) suggests that these two ages should represent the same interval of continuous growth. Core D4 grows continuously also between ca. 81.1 ± 2.6 ka and 75.0 ± 0.8 ka. Growth in the terminal part of the two cores is disturbed by a series of interruptions, none of which are fully chronologically constrained but with clear evidence in thin section of erosion and mud deposition (Regattieri et al., 2012). Two ages indicate discontinuous growth at ca. 12.6 ± 0.7 ka and 7.8 ± 0.3 ka.

The growth rate in D4 (Fig. 5) shows initial values of ca. 8.8 mm/ka followed by a peak of 10.5 mm/ka at ca. 153.5 ± 1.9 ka. This peak is succeeded by a very low growth rate (average ca. 3.3 mm/ka) until ca. 130 ka, after which it increases dramatically to up to ca. 20 mm/ka (between ca. 130 and 127 ka). After ca. 127 ka, the growth rate decreases abruptly in two subsequent steps: until ca. 9 mm between ca. 126 and 125 ka and then to 3–3.5 mm/ka from ca. 124 ka to the Hs1.

Stable isotopes

The δ^{13}C and δ^{18}O variations measured in D4 and D3 vs. depth from top (mm) are shown in Figure 4, whilst the stable isotope composition vs. age for the discussed section of D4 is displayed in Figure 5. The δ^{18}O values range from −2.79‰ to −6.28‰ in D4 and from −2.47‰ to −6.32‰ in D3, whilst the δ^{13}C values range from −2.24‰ to −10.74‰ in D4 and from −1.04‰ to −10.69‰ in D3. Isotope profiles from the lower section of both cores show substantially the same pattern of variations, although sometimes with different degrees of compression (vs. distance) for the same oscillations. The record starts with δ^{18}O values of ca. −3.8 ‰ and there is a peak of lower values (average ca. −4.5‰) which starts at ca. 154.0 ± 2.0 ka and terminates

https://doi.org/10.1016/j.yqres.2014.05.005 Published online by Cambridge University Press

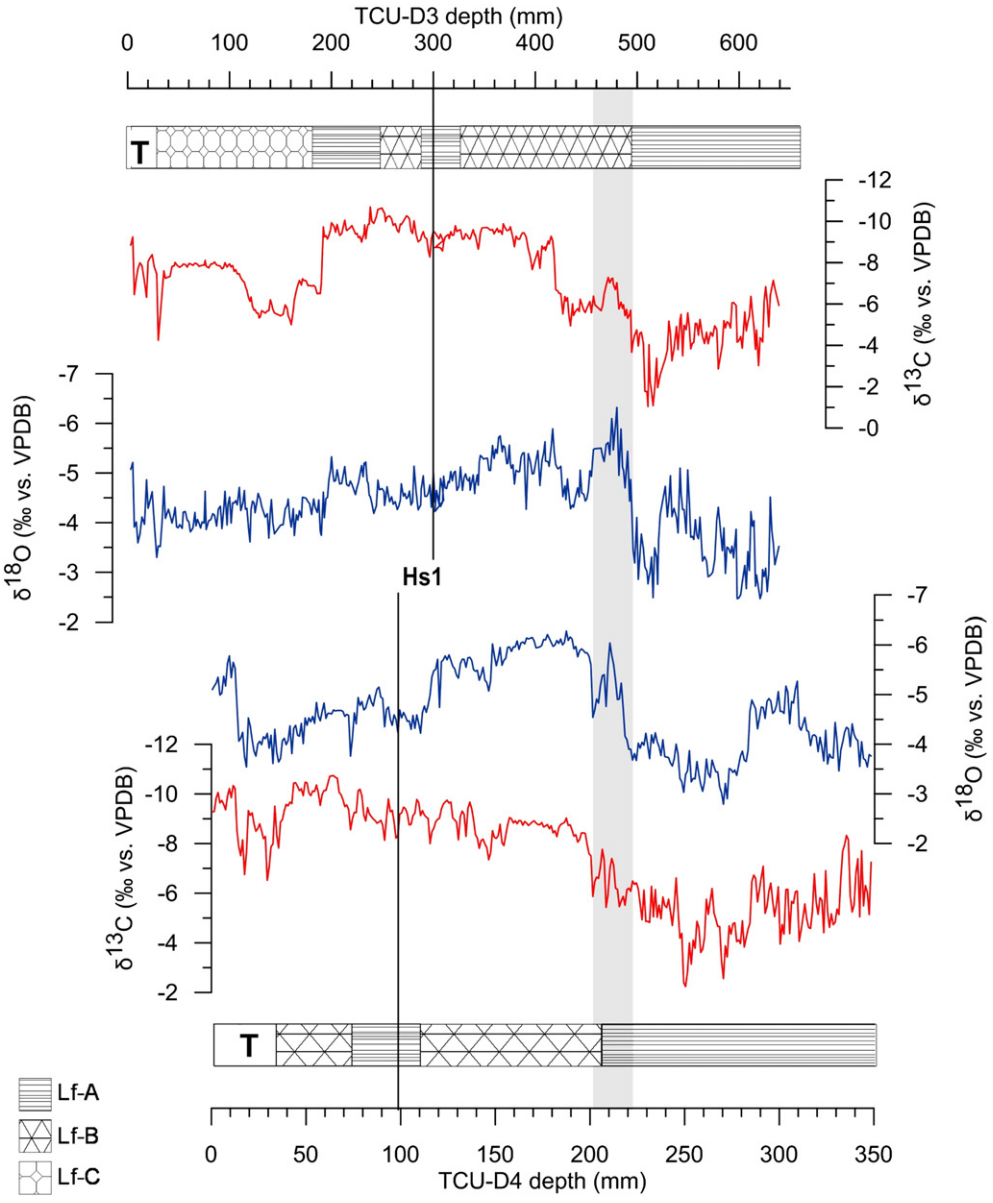

Figure 4. Stable isotope compositions and lithofacies (from Regattieri et al., 2012) vs. depth from top (mm) of cores D3 (top) and D4 (bottom) ($\delta^{13}C$ in red, $\delta^{18}O$ in blue). Black line marks the hiatus Hs1 and shaded area highlights the excursion corresponding to glacial/interglacial transition. See main text for details.

abruptly around ca. 151.6 ± 2.2 ka. Thereafter follows an interval of generally higher values between ca. 151.4 ± 1.9 and ca. 132.2 ± 1.2 ka, with consistent millennial variability ($\delta^{18}O$ difference of average 0.7‰) and a slight trend towards lower values from ca. 139.9 ± 2.7 ka. The most prominent feature of the oxygen record, however, starts at ca. 132.1 ± 1.8 ka, when a dramatic excursion of ca. 3 ‰ towards lower values occurs, which peaks at ca. 131.0 ± 1.2 ka. A narrow and sharp positive peak centered at ca. 129.6 ± 1.0 ka is followed by the interval of lowest values, which lasts between ca. 129.4 ± 1.0 and 126.7 ± 1.2 ka. At ca. 126.1 ± 1.3 ka there is another excursion to higher values (ca. 0.7 ‰) lasting ca. 0.9 ka, and then an interval of lower values which persists until ca.123.6 ± 1.2 ka. After this interval in both cores the $\delta^{18}O$ values increase sharply (ca. 1.2 ‰) and then remain stable until hiatus Hs1 (ca. 121.4 ± 2.0 ka) which marks the end of the discussed interval.

The $\delta^{13}C$ record closely follows the major changes in $\delta^{18}O$, that is, all of the prominent features of oxygen are marked by in-phase variations of $\delta^{13}C$ (Figs. 4 and 5). The r^2 values (covariation between $\delta^{18}O$ and $\delta^{13}C$ along the growth axis) are 0.33 and 0.36 for D4 and D3, respectively. For the sharp excursion at ca. 132.1 ka, the total $\delta^{13}C$ change is about 3.6‰. Close to the end of the discussed interval, it is possible to observe a slightly different behavior for the two records: at ca. 126.5 ka the $\delta^{13}C$ shows the same positive oscillation previously described for the $\delta^{18}O$ but it is longer and less prominent. After this, the carbon isotopes return to previous values and steadily decrease until hiatus Hs1, whereas the oxygen after ca. 126.5 ka only consistently increases.

Discussion

The Tana che Urla proxy record (stable isotope and growth rate, Fig. 5) shows a consistent pattern of variability at both orbital (i.e. glacial–interglacial transition) and suborbital time scales (centennial-to-millennial scale). There is also a persistently good correspondence between the isotopic record (especially for oxygen), growth rate and petrographic change in the cores: the white, clastic-poor calcite occurs during periods of prevailing lower isotope values and higher growth

https://doi.org/10.1016/j.yqres.2014.05.005 Published online by Cambridge University Press

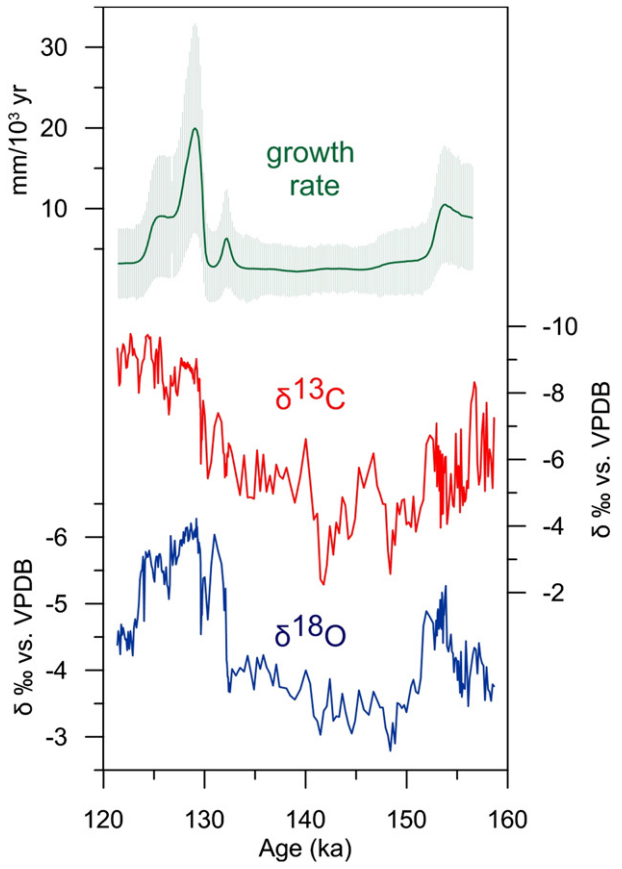

Figure 5. Stable isotope and growth rate time series for the ca. 159–121 ka section of core D4. The growth rate time series is derived from age–depth modelling (see Hellstrom, 2006), the envelope represents the 2σ uncertainties.

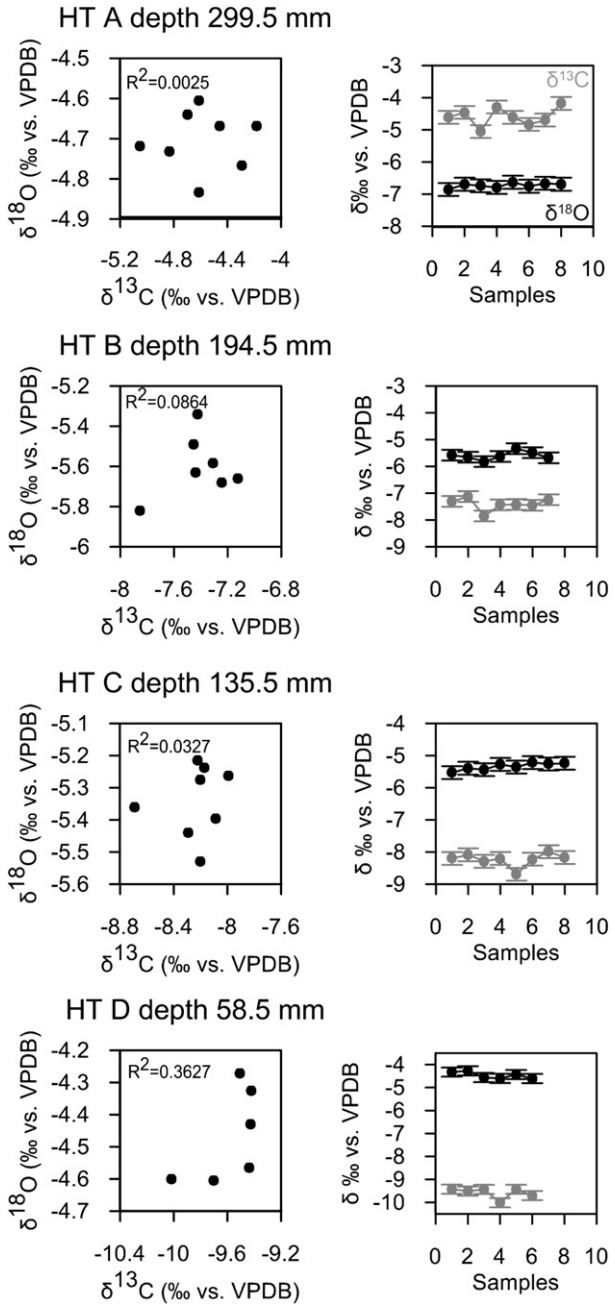

Figure 6. Results of Hendy tests performed on core D4. Right panel: $\delta^{13}C$ in grey, $\delta^{18}O$ in black.

rates, while the brown, clastic-rich calcite occurs principally during periods of lower growth rate and higher isotope values.

Equilibrium deposition

In the recent literature, it has been recognized that kinetic isotopic effects are present in many speleothem records (e.g. Mickler et al., 2006; Wainer et al., 2011). "Hendy tests" are the classical tools used to test whether calcite from a given speleothem was deposited out of isotopic equilibrium (Hendy, 1971). We have applied this test to four flowstone laminae to check the isotopic composition behavior laterally. Each case shows no significant correlation between $\delta^{18}O$ and $\delta^{13}C$ and almost constant values of $\delta^{18}O$ and $\delta^{13}C$ along a single growth layers (Fig. 6), suggesting equilibrium or quasi-equilibrium deposition (Hendy, 1971). However, Hendy tests are no longer viewed as definitive proof of isotopic equilibrium (e.g. Mühlinghaus et al., 2009; Day and Henderson, 2011) and so further evidence of near-equilibrium deposition is required. Recent literature (e.g. Dorale and Liu, 2005; Fairchild and Baker, 2012) suggests that near-equilibrium deposition is likely if the isotopic patterns of two or more coeval samples from the same cave reproduce favorably. For the TCU flowstone, comparison between the two stable isotope records of D4 and D3 shows that they are remarkably similar over the contemporaneous growth period, providing a robust replication test (Fig. 4, e.g. Dorale and Liu, 2005; Fairchild and Baker, 2012). The small discrepancy between the two records may indicate minor kinetic effects and/or the influence of different growth rates for the two lobes of the flowstone from which the cores were taken, but these differences are small compared to the overall range of values (e.g. for oxygen the biggest excursion corresponding to MIS6/MIS6 transition is from −3.68 to −6.04‰ on D4, whereas it is from −2.86 to −6.32‰ for D3), suggesting that changes in the $\delta^{18}O$ are driven by changes in the $\delta^{18}O$ of meteoric water and cave temperature. Moreover, the monotonous columnar fabric is believed to occur when speleothems are continuously wet, and from fluids at near-isotopic equilibrium conditions with low oversaturation (Frisia et al., 2000).

Equilibrium conditions can also be inferred theoretically, in particular using data from modern cave-water monitoring. Water samples collected randomly from several drip sites over three years show average $\delta^{18}O_w$ values of −7.13 ± 0.27‰ (n = 7). Average $\delta^{18}O$ values for calcite from the top section of D4 and deposited over the Holocene – a period of relatively little paleoclimate change – are −5.23‰ ± 0.2‰. Using the

https://doi.org/10.1016/j.yqres.2014.05.005 Published online by Cambridge University Press

Kim and O'Neill (1997) equation for isotopic fractionation coefficient, we obtain an equilibrium temperature of 7.5°C (±1.5°C), which is somewhat lower that the modern interior cave temperature (10.2°C). However, results from a compilation of published cave monitoring data show a frequent ^{18}O-enrichment of 0.5–1‰ in speleothem calcite compared to the isotopic equilibrium value (McDermott et al., 2006). Although it has yet to be demonstrated that this enrichment is not due to a modest kinetic effect, the temperature inferred for Holocene calcite considering this offset would range from 11.9 to 10.2°C, values which are closer to the modern cave temperature. Although only approximations, these calculations provide additional evidence of ~-equilibrium deposition for TCU flowstone.

It is possible to estimate the $\delta^{13}C$ values of speleothem calcite that would have precipitated in equilibrium with seepage waters knowing the $\delta^{13}C$ values of DIC. The few data available on drips and pool waters from TCU give an average value of -10.0 ± 1.5‰ ($n = 4$). Considering the isotopic fractionation factor between $CaCO_3$ and HCO_3^- of ca. 1‰ (Romanek et al., 1992), calcite precipitated in equilibrium would have values of ca. −9.0‰, close to observed values for the Holocene (-9.6 ± 0.3‰) and minimum values of the Last Interglacial (-8.6 ± 0.3‰). The small differences can be accounted by a small degree of kinetic isotopic fractionation and/or exchange with cave CO_2 (e.g. Oster et al., 2010; Tremaine et al., 2011). Following the approach of Oster et al. (2010), it is possible to estimate the extent of processes affecting the isotopic composition of the dissolved inorganic carbon of water equilibrated with soil CO_2 and the final carbon isotope composition of speleothem calcite. After equilibration with soil CO_2, DIC isotopic composition evolves due to the different contributions of bedrock and other processes, such as prior calcite precipitation (e.g. Fairchild et al., 2006 and references therein). In this approach, the isotopic composition of soil litter is assumed to be close to the isotopic composition of soil CO_2, taking into account fractionation of 4.4‰ caused by differing diffusion coefficients for $^{12}CO_2$ and $^{13}CO_2$ (Cerling et al., 1991) and a coefficient between HCO_3^- and $CO_{2(g)}$ of ca. + 9‰ (Zhang et al., 1995). Litter samples collected above the cave between 650 and 900 m asl show average values of -27.4‰ ± 1.3‰ ($n = 7$) (Berti, 2010). This allows us to estimate a value of DIC in equilibrium with local soil CO_2 of ca. −13‰. The ca. 3‰ difference between this value and the DIC measured in the cave can be explained by the contribution from the dissolution of the host bedrock, prior degassing and prior calcite precipitation (Oster et al., 2010) and/or closed-to-open-system evolution of the DIC compared to soil CO_2 and/or mineralization of different organic matter soil components (e.g. Rudzka et al., 2011). Although these calculations can contain large errors, they are consistent with the isotopic composition of the TCU speleothems being close to the water DIC $\delta^{13}C$ values. This suggests that changes in the $\delta^{13}C$ values of DIC are mostly related to variations in soil CO_2 equilibration.

Therefore, there are sufficient arguments to sustain the notion that the isotopic variability observed in the two TCU cores is not dominated by kinetically induced disequilibrium fractionation during calcite precipitation. We thus believe that the TCU isotope time series mainly reflect changes in the $\delta^{18}O$ of meteoric water and/or cave temperature.

Paleohydrological significance of $\delta^{18}O$ and growth rate

For Mediterranean speleothems, atmospheric condensation temperature effects are likely to be balanced by changes in cave temperature (e.g. Bar-Matthews et al., Bard et al., 2002; Drysdale et al., 2004; Zanchetta et al., 2007) and therefore changes in speleothem $\delta^{18}O$ calcite are thought to reflect principally changes in the isotopic composition of $\delta^{18}O$ of meteoric precipitation due to the "amount effect" (e.g. Dansgaard, 1964) and/or to changes in $\delta^{18}O$ of ocean surface water ("source effect") due largely to ice-volume changes. This conclusion was first proposed by Bar-Matthews et al. (1999, 2000, 2003) for the eastern Mediterranean (Soreq Cave, Israel). Subsequently, it has been suggested that for eastern Mediterranean at glacial/interglacial transition, the influences of rainfall amount, sea–land distance and elevation changes related to sea level changes are superimposed on ocean-surface water $\delta^{18}O$ changes, brought about by continental ice melting (Bar-Matthews et al., 2003; Kolodny et al., 2005; Almogi-Labin et al., 2009). Instead, during interglacial periods, the amount effect is considered dominant. On the other hand, for the western Mediterranean, Bard et al. (2002) examined data from the GNIP-IAEA stations of Genoa, Palermo and Pisa and analyzed the inter-annual variations of $\delta^{18}O_p$ and atmospheric temperature. They showed that $\delta^{18}O_p$ and temperature are positively correlated, with a slope of +0.3‰/°C, which is close in magnitude but opposite in sign to the cave-temperature effect (−0.24‰/°C). More significantly, they found that $\delta^{18}O_p$ is also anticorrelated with the amount of precipitation, with a slope of −2‰ per 100 mm/month. Isotopic modelling performed by Bard et al. (2002) indicated that for the western Mediterranean this effect should be dominant in glacial, interglacial and intermediate climate states. During the deglaciation, the amount effect is clearly superimposed on the effect of changes in the $\delta^{18}O$ of sea water, both in the Mediterranean and in the North Atlantic, which in turn depend on changes in the global ice volume (i.e. lower $\delta^{18}O$ composition of sea water due to ice melting) as well as on changes in the freshwater budget for Mediterranean, and from evaporation in the tropics and patterns of ocean-water circulation for the North Atlantic (Kallel et al., 2000). Although the relative importance of each effect is difficult to evaluate, they each act in the same direction as the amount effect (i.e. decreasing $\delta^{18}O$ composition of rainfall during the deglaciation).

These considerations have been used to interpret the isotopic records of nearby Corchia Cave (Fig. 1), and changes in the amount precipitation inferred from oxygen isotopes from this archive were interpreted due to changes in advection of moisture from Atlantic in response to changes in the strength of MOC (e.g. Drysdale et al., 2004, 2007; Zanchetta et al., 2007). The notion that the $\delta^{18}O$ of speleothem calcite in this area mostly retains information on changes in paleorainfall amount has been supported by trace element and/or growth rate data at Corchia (Drysdale et al., 2009; Regattieri et al., 2014), and Mg and organic fluorescence patterns at the lower-altitude Renella Cave (Drysdale et al., 2006). At Renella Cave, major alluvial phases are in phase with lower $\delta^{18}O$ values at Corchia during the Holocene (Zhornyak et al., 2011). Thus, it is reasonable to assume that in TCU, speleothem $\delta^{18}O$ is also mainly driven by the "amount effect" on precipitation related to North Atlantic conditions.

The observed variations in the growth rate of the TCU flowstone (Fig. 5) and their potential relationship to hydrological changes should be interpreted with caution because they relate only to one flowstone, and it is reasonable to expect that different parts of the cave may yield differing speleothem growth patterns as fractures widen, narrow, and close over time. However, the changes in growth rate are consistent with the proposed interpretation for stable isotope variations (i.e. higher growth rate during periods of enhanced precipitation), supporting the inferences that they, too, are climate-related.

MIS 6 variability and the transition to the Last Interglacial

The basal section of the flowstone, from ca. 159.1 ± 1.3 to 132.2 ± 1.8 ka, shows higher $\delta^{18}O$ values and lower growth rates (Fig. 5) indicating generally drier conditions. The interval between 160 and 130 ka corresponds to late MIS 6, when a large ice sheet covered northern Europe (e.g., Imbrie et al., 1984). This period has been the subject of several studies (e.g. Rossignol-Strick, 1983, 1985; Cheddadi and Rossignol-Strick, 1995; Ayalon et al., 2002; Bard et al., 2002), most of which indicate that conditions through the entirety of MIS 6, even during the coldest events, were relatively humid in comparison to MIS 4–2 (Ayalon et al., 2002). Although resolution and age control through the MIS 6 section of our record preclude a detailed discussion, it is notable that flowstone growth at TCU during at least the last part of MIS 6 was continuous, whereas the last glacial was characterised by several growth interruptions, suggesting

https://doi.org/10.1016/j.yqres.2014.05.005 Published online by Cambridge University Press

a more severe climate. Furthermore, a prominent phase indicative of enhanced rainfall is centered at ca. 153.1 ± 1.9 ka and also corresponds to a phase of higher growth rate. This excursion lasts ca. 2 ka and terminates quite abruptly. It may correspond to a wetter period identified in Soreq Cave (Israel) speleothems, centered at ca. 152 ka (Ayalon et al., 2002). This interval is very prominent in the Soreq Cave record and is thought to correspond to the *G. ruber* $\delta^{18}O$ minimum from eastern Mediterranean marine cores (e.g., Vergnaud-Grazzini et al., 1977; Bar-Matthews et al., 2003) and to be most probably equivalent to the monsoon index maxima ca. 151 ka (e.g. Méliéres et al., 1997). Interestingly, a similar period of enhanced precipitation around 150 ka, indicated by a small $\delta^{18}O$ anomaly, was recognized also in the speleothem record from Argentarola Cave (Southern Tuscany, Bard et al., 2002), where it was linked to the insolation maximum at 150 ka.

At ca. 132.1 ± 1.8 ka all speleothem properties show a relatively abrupt and high-amplitude change: oxygen and carbon values decrease rapidly, the growth rates dramatically increase (passing from average values of about 4 mm/ka to ca. 20 mm/ka) and the brown, clastic calcite is replaced by the white clastic-poor lithofacies (Regattieri et al., 2012). The $\delta^{18}O$ record indicates progressively enhanced precipitation over the cave catchment at this time, marking the transition between the penultimate glacial and the last interglacial (i.e. the MIS 6 to MIS 5 transition in marine records). Within age error, the TCU $\delta^{18}O$ is consistent with the $\delta^{18}O$ record from Corchia Cave (Drysdale et al., 2005, 2009, Figs. 1, 7, and 8). Similarities with the oxygen record from Soreq Cave are also evident (Bar-Matthews et al., 2003, Figs. 1 and 7).

Within age error, the TCU record is also in agreement with reconstructions of vegetation changes occurring throughout the deglaciation from marine core MD95-2042 (Iberian margin, southwestern Europe, Sánchez Gõni et al., 1999; Sanchez-Goni, 2005, Figs. 1 and 7), and slightly precedes the glacial–interglacial transition in the Monticchio Lake pollen record (Brauer et al., 2007; Allen and Huntley, 2009, Figs. 1 and 7). Both pollen records show an increase in woody mesic taxa through the deglacial, which suggests not only a wetter but also a warmer climate. This is also supported by alkenone-derived SSTs from marine core ODP-977A (Martrat et al., 2007, Figs. 1 and 7).

Suborbital variability of MIS 5e

The TCU $\delta^{18}O$ record shows significant multi-centennial variability between the peak interglacial conditions at ca. 131.0 ka and hiatus Hs1 at ca. 121.4 ka. The lowest isotope values occurred between ca. 131.0 and 123.6 ka, indicating that the wettest period lasted ca. 6 ka. However, this period is interrupted by two short prominent events, indicating reduced precipitation between ca. 130.7 and 129.6 ka and between ca. 126.7 and 125.6 ka. After 123.6 ka, values again increase abruptly then remain stable until hiatus Hs1. The regional significance of these events can be evaluated by comparing the TCU record with other archives. The TCU and Corchia records display remarkable similarities also for MIS 5e (Figs. 7, 8 and 9) whilst an even greater degree if similarity is evident with a speleothem record from western France (Bd-inf, Fig. 9, Bourgeois-Delaunay Cave, Couchoud et al., 2009). The event at ca. 126.7-125.6 ka and another from ca. 123.6 ka to hiatus Hs1 are well expressed in all the three records (Fig. 9). Also, cores from two well-studied North Atlantic sites, ODP980 (sub-polar North Atlantic, McManus et al., 1999, 2002; Oppo et al., 2001, 2006; Fig. 1) and ODP1059 (Sub-tropical western North Atlantic, Oppo et al., 2001, 2006; Heusser and Oppo, 2003; Fig. 1), display two intra-Eemian (or intra-MIS5e) cooling events, labelled C28 and C27 (at ca. 129 and 122 ka respectively, Oppo et al., 2001). ODP980 and ODP1059 sites are sensitive to changes in MOC in the North Atlantic Ocean, which in turn affects westward moisture advection and, as previously discussed, precipitation amount in the Mediterranean basin. In these marine cores, the C29 and C28 events slightly follow the glacial termination and thus could be correlated respectively with the event of reduced moisture at ca. 129.6 ka and with that starting at ca. 123.6 ka on D4 $\delta^{18}O$ record. The event at ca. 126.5–125.6 ka does not seem to have an obvious correlation with sub-polar and western North Atlantic marine cores, although correlation of these events is problematic due to the intrinsically different age models

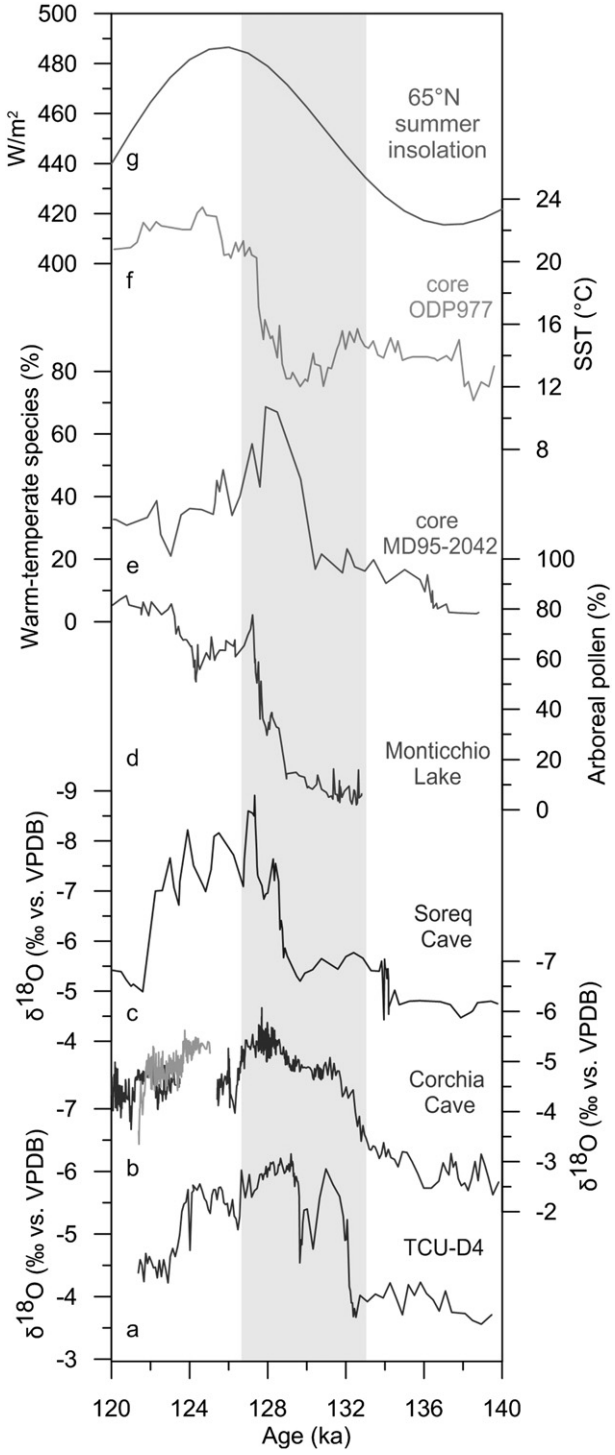

Figure 7. Comparison between $\delta^{18}O$ of core D4 (a) and $\delta^{18}O$ of Corchia Cave (b), stalagmites CC5 blue, CC7 light blue, (Drysdale et al., 2009), $\delta^{18}O$ of Soreq Cave (c, Bar-Matthews et al., 2003), percentage of arboreal pollen at lake Monticchio (d, Brauer et al., 2007; Allen and Huntley, 2009). percentage of warm and temperate species from Iberian-margin marine core MD95-2042 (e, Sánchez Gõni et al., 1999; Sanchez-Goni, 2005), alkenone-based sea-surface temperatures from western Mediterranean core ODP-977A (f, Martrat et al., 2004) and June insolation at 65° N (g, Berger and Loutre, 1991). All records are reported on their own published age models. Grey shading highlights the outer range of the excursion corresponding to glacial–interglacial transition.

https://doi.org/10.1016/j.yqres.2014.05.005 Published online by Cambridge University Press

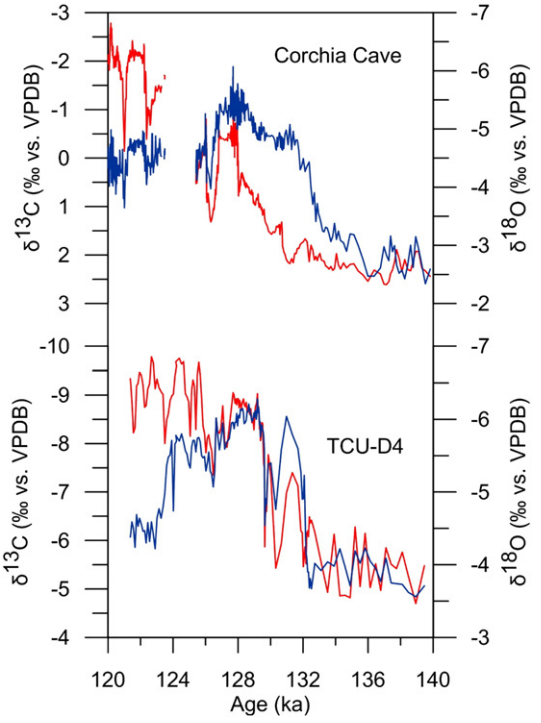

Figure 8. Comparison of $\delta^{18}O$ and $\delta^{13}C$ between TCU core D4 and Corchia Cave (stalagmite CC5, Drysdale et al., 2005, 2009).

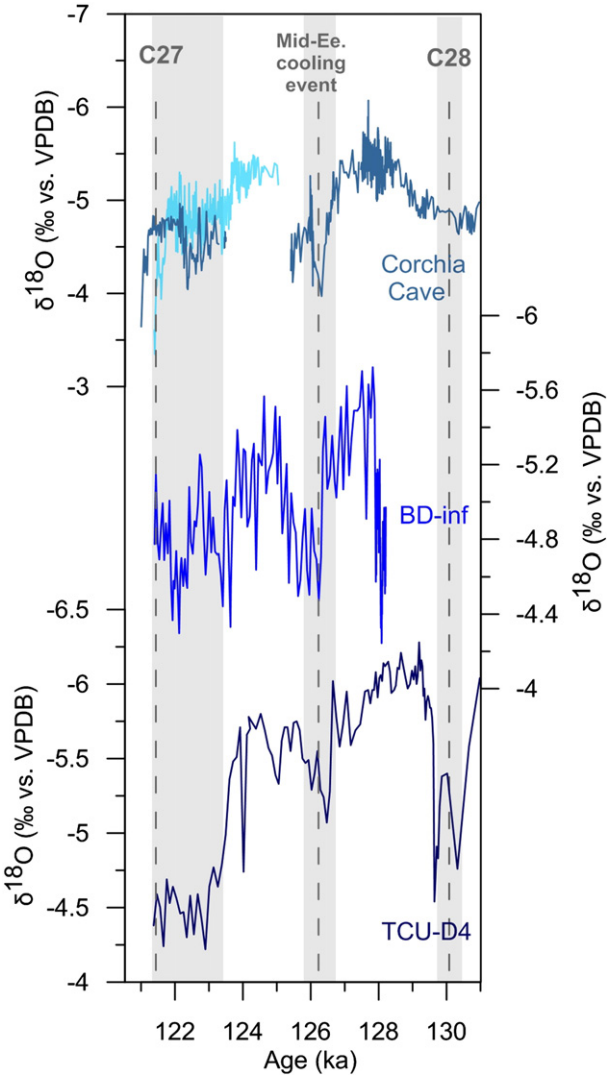

Figure 9. Comparison of MIS5e variability from $\delta^{18}O$ of core D4, $\delta^{18}O$ of stalagmite BD-inf (Bourges-Delauny Cave, Couchoud et al., 2009) and $\delta^{18}O$ of Corchia Cave (stalagmites CC5 blue and CC7 light-blue, Drysdale et al., 2005, 2009). Grey shading indicates drier intervals from D4 record, grey dashed lines indicate C28 and C29 cold events from Oppo et al. (2001) and the middle-Eemian cooling event from marine core MD95-2042 (Sánchez Gõni et al., 1999, 2007).

of speleothems and marine cores, and also to the discrepancy in resolution between the different records.

Interestingly, the $\delta^{18}O$ values of TCU after the second event (from ca. 126.5 ka) remain more positive than the early LIG (130–127 ka), thus suggesting that the wettest part of MIS5e in the area occurred in the earliest part of the interglacial.

Correlations between two North Atlantic cores (ENAM33 and MD95-2009, Fig. 1) from south and north of the Iceland–Scotland Ridge demonstrate that during the MIS 6/5e transition, the polar front was displaced ca. 1000 km to the southeast compared to the present day, and that sea-surface temperatures rose 3000 years earlier south of the ridge (ca. 130 ka) than north of the ridge (ca. 127 ka) (Rasmussen et al., 2003). Whereas NADW formation and, more generally, North Atlantic MOC were not affected by cold surface conditions in the Norwegian Sea before 127 ka, cold surface water conditions in the Nordic seas can be assumed to have had a negative effect on cyclonic activity in this region (Rasmussen et al., 2003). This implies a reduction of the westerly wind intensity over NW Europe (Rasmussen et al., 2003). For the Holocene, it has been suggested that reduction in the intensity of the westerlies results in increased precipitation over the Mediterranean basin, because the northward transport of vapor masses sourced from the subtropical sector of the North Atlantic is less efficient and therefore part of this moisture can penetrate the basin interior instead of being transferred to NW Europe (Fletcher et al., 2012). We suggest that the apparent reduction in precipitation recorded at TCU (but also in Corchia record, Fig. 9) from ca. 127 ka could reflect surface warming of the Nordic seas, producing enhanced cyclonic activity, stronger westerlies and a more efficient transport of vapour masses towards NW Europe. This is supported also by the occurrence of a mid-Eemian wet and cold period in core MD95-2042 around 126.5 ka, so substantially synchronous with the second oxygen-depleted event in TCU record, which was presumably related to southward displacement of the Polar Front, favoring the formation of major atmospheric depressions and enhanced cyclonic activity over the North Atlantic and western-southern Europe (Sánchez Gõni et al., 1999).

Interpretation of $\delta^{13}C$ record

While the $\delta^{18}O$ signal at Tana che Urla can be linked to regional-scale climatic conditions, the $\delta^{13}C$ record gives more detailed information into local environmental changes, even if it strictly follows the $\delta^{18}O$ signal, indicating a strong sensitivity to regional climate change. Interpretations of speleothem $\delta^{13}C$ records are challenging because of the complex reactions involving soil CO_2, bedrock dissolution, and the reaction kinetics in the CO_2-H_2O-$CaCO_3$ system (e.g. Fairchild and Baker, 2012). Many processes, however, tend to drive the final $\delta^{13}C$ of speleothem in the same direction. For instance, elevated values of speleothems can be due to a decrease in soil-CO_2 productivity (e.g. Genty et al., 2001, 2003), usually associated with a reduction in rainfall and cooler climate. Reduction in recharge can also produce degassing along the fracture paths, with enhanced calcite precipitation occurring before drip waters reach the cave (e.g. Baker et al., 1997; Fairchild et al., 2006). In this view, higher $\delta^{13}C$ values of the calcite between ca. 159 and 132 ka, representing the glacial period of MIS 6, are consistent

https://doi.org/10.1016/j.yqres.2014.05.005 Published online by Cambridge University Press

with a reduction in soil vegetation and respiration rates due to cooling and/or reduced recharge.

Regional pollen records for central and Southern Italy (e.g. Follieri et al., 1988; Brauer et al., 2007; Allen and Huntley, 2009) indicate rapid forest expansion at the transition from MIS 6 to MIS 5. Accordingly, the observed $\delta^{13}C$ variation during the glacial to interglacial transition in TCU suggests forest expansion, soil development and enhanced soil CO_2 production during the climate transition, leading to a decrease in the speleothem $\delta^{13}C$. The synchronicity between the $\delta^{18}O$ and $\delta^{13}C$ in TCU (Figs. 4 and 8) indicates that changes in soil conditions in the TCU catchment happened not only relatively quickly but in sync with the increase in rainfall, reaching interglacial values within ca. 2000 yr.

To understand the rapid responses of soil development above TCU Cave, a comparison with the Corchia Cave $\delta^{13}C$ record for the same interval is useful, and provides insights into the differences in soil evolution above each cave (Fig. 8). At the glacial–interglacial transition, the $\delta^{13}C$ of Corchia Cave speleothems shows a lagged (ca. 2000 yr) and more gradual shift to lighter values compared to $\delta^{18}O$, owing to the time required for post-glacial soils to establish above Corchia (Drysdale et al., 2004, 2005, 2009; Zanchetta et al., 2007). The present physiographic setting of the two caves is quite different: Corchia Cave is a large (ca. 60 km) and deep (1187 m below surface) karst system. The recharge area of the well-studied deep chamber "Galleria delle Stalattiti (from where all the published speleothem records are derived so far) is located between 1200 and 1400 m asl (Piccini et al., 2008) and it is dominated by very steep terrain of mostly bare, high-purity bedrock, with only occasional soil-filled solution features and little vegetation cover. The high $\delta^{13}C$ values in drip water and speleothems in Corchia (Piccini et al., 2008; Baneschi et al., 2011) suggest a low input of biogenic CO_2 (Dulinski and Rozanski, 1990), having $\delta^{13}C$ values of DIC of ca. −3.36‰ (SD 0.15‰) (Baneschi et al., 2011). This is in agreement with the poorly developed soil cover and deep location of the chamber, which promote a greater contribution from bedrock carbon, which has values between −0.5 and +1.7 ‰ (range of values for the Grezzoni formation, average +0.8 ± 0.9‰, Cortecci et al., 1999). The $\delta^{13}C$ of soil organic matter collected above Corchia between ca. 1200 and 1400 m asl shows values of −26.25 ± 1.54‰ (Berti, 2010). Performing the same calculation as that for TCU, a DIC in equilibrium with soil CO_2 should have values of around −12.85‰. The very large difference from these calculated values and the DIC $\delta^{13}C$ values obtained in the Galleria delle Stalattiti indicates a greater contribution of bedrock (including dissolution due to pyrite weathering, as suggested by chemical mass balance calculations — our unpublished data) and, additionally, other effects like prior calcite precipitation and mixing of solutions having different degrees of evolution (Regattieri et al., 2014). In contrast, Tana che Urla is a small, shallow cave, and the recharge area is covered by a relatively deep soil and sustains a well-developed forest. $\delta^{13}C$ values in calcite and DIC are very low with respect to Corchia, and, as suggested above, indicate a predominance of a biogenic component in cave water CO_2 and most importantly in the $\delta^{13}C$ signal of the speleothem (Fig. 8).

Owing to the present setting of TCU Cave, its continuous speleothem growth during late MIS 6 and the low absolute values of $\delta^{13}C$ in glacial calcite (even below those of Corchia interglacial values), we speculate that soils in the infiltration area of TCU were relatively well developed even during the last part of the penultimate glacial. A certain degree of soil development would allow a rapid recovery of vegetation once climatic amelioration commenced during the glacial–interglacial transition. The simultaneous changes in oxygen and carbon values observed at TCU can also explain the apparent age discrepancies between the TCU and Monticchio records for the LIG: at Lake Monticchio, the transition from the preceding glacial, evident in both the palaeovegetation record and the sediment lithology, began at ca. 130.55 ka, extending over a 3.35-ka period, with the ultimate onset of the interglacial placed at ca. 127.2 ± 1.4 ka (Brauer et al., 2007; Allen and Huntley, 2009). In TCU record, the transition starts at ca. 132.1 ± 1.8 ka (well within age error of Monticchio) and ends at ca. 131.0 ± 1.2 ka, perhaps lasting less than a thousand years. Because changes in taxa due to plants colonizing from refugia may have a significant inertia, the age offset between the two records for the onset of full interglacial conditions may therefore simply reflect different response times of different proxies (pollen vs. isotopes) to a simultaneous climatic forcing.

Conclusions

The growth history and stable isotope geochemistry of two cores from Tana che Urla (Alpi Apuane central-western Italy) preserve a continuous record from the latter part of the penultimate glacial to the middle part of the last interglacial (ca. 159–121 ka), and captures both orbital-scale (i.e. glacial/interglacial transition) and sub-orbital climate variability. The most prominent feature of the record is the dramatic excursion towards lower isotope values at ca. 132 ka, coincident with a change in the lithology (from brown, detrital-rich to white, detrital-poor calcite) and a fourfold increase in flowstone growth rate. The shift in all speleothem properties implicates enhanced rainfall in the recharge area, related to climatic amelioration at the glacial/interglacial transition, and agrees (within age errors) with the principal structural features of others speleothem and pollen records from central Italy (Drysdale et al., 2005, 2009; Follieri et al., 1988; Allen and Huntley, 2009; Brauer et al., 2007) as well as with regional SST reconstructions (Martrat et al., 2004, 2007). Interestingly, at TCU the shift in $\delta^{13}C$ and $\delta^{18}O$ corresponding to glacial–interglacial transition is substantially synchronous, while at nearby Corchia Cave (Drysdale et al., 2005, 2009; Zanchetta et al., 2007) there is a lag of ca. 2 ka of the shift in $\delta^{13}C$ with respect to $\delta^{18}O$. At Corchia Cave, this was interpreted as due to the time lag needed for soil recovering in the high-altitude catchment area (ca. 1200 m asl). Instead, at TCU the contemporaneous decrease in both isotope records suggests that soils in the infiltration area (ca. 600–700 m asl) were relatively well developed even during the last part of the penultimate glacial, allowing a rapid recovery of vegetation once climatic amelioration commenced during the glacial–interglacial transition.

During late MIS 6, we observe slower growth rates and higher isotope values, suggesting generally cooler–drier conditions, interrupted by a peak towards more negative isotope values and higher growth rates between ca. 154.0 and 151.6 ka. This peak is interpreted as a humid period and it is coincident with similar conditions inferred from speleothem records from Israel (Ayalon et al., 2002) and southern Tuscany (Bard et al., 2002). Further, the interglacial part of the record shows substantial variability, with three events of reduced moisture at ca. 129.6, 126.0 ka and between 123.6 ka and the first growth interruption at ca. 121.4 ka. This climatic instability during the first part of the last interglacial substantially agrees with the nearby speleothem record from Corchia Cave (Drysdale et al., 2005, 2009) and matches the occurrence of cold and dry events recognized in a speleothem record from western France (Couchoud et al., 2009), suggesting a regional expression of these events and firmly anchoring their cause to circulation changes in the adjacent North Atlantic. This idea is further supported by the correlation among the first and the third events recorded at Tana che Urla and two cold events (C28 and C27 at ca. 122 and 129 ka) recorded in North Atlantic marine cores (e.g. Oppo et al., 2001). The second event has no obvious correlation with the North Atlantic record but may coincide with a mid-Eemian cool and wet period identified in the pollen record from marine core MD95-2042 at ca. 126 ka (Sánchez Gõni et al., 1999; Sanchez-Goni, 2005), inferred to be due to increased cyclonic activity over western Europe driven by southward displacement of the polar front. The presence of major atmospheric depressions in the sub-polar North Atlantic is thought to be responsible for more efficient vapor-mass transport towards northern and western Europe (Fletcher et al., 2012), leading to less effective penetration of major cyclonic perturbations in the Mediterranean basin and reduced precipitation at TCU.

https://doi.org/10.1016/j.yqres.2014.05.005 Published online by Cambridge University Press

Acknowledgments

Financed by the Australian Research Council Discovery Project scheme (grant number DP110102185). ER is supported by a PhD grant of the School of Graduate Studies Galileo Galilei (University of Pisa). We thank the Federazione Speleologica Toscana and Parco Apuane for supporting our work on Apuan Alps speleothems. We thank I. Baneschi, M. Guidi, C. Boschi and L. Dallai for unpublished isotopic data on Tana Che Urla waters, obtained within collaboration in monitoring cave waters on Apuan Alps. We also thank two anonymous reviewers and the associated editor for their comments and suggestions, which improved the quality of the manuscript.

References

Allen, J.R.M., Huntley, B., 2009. Last Interglacial palaeovegetation, palaeoenvironments and chronology: A new record from Lago Grande di Monticchio, southern Italy. Quaternary Science Reviews 28, 1521–1538.

Almogi-Labin, A., Bar-Matthews, M., Shriki, D., Kolosovsky, E., Paterne, M., Schilman, B., Matthews, A., 2009. Climatic variability during the last ~ 90 ka of the southern and northern Levantine Basin as evident from marine records and speleothems. Quaternary Science Reviews 28, 2882–2896.

Ayalon, A., Bar-Matthews, M., Kaufman, A., 2002. Climatic conditions during marine isotope stage 6 in the eastern Mediterranean region from the isotopic composition of speleothems of Soreq Cave, Israel. Geology 30, 303–306.

Baker, A., Barnes, W.L., Smart, P.L., 1997. Variations in the discharge and organic matter content of stalagmite drip waters in Lower Cave, Bristol. Hydrological Processes 11, 541–555.

Baneschi, I., Piccini, L., Regattieri, E., Isola, I., Guidi, M., Lotti, L., Mantelli, F., Menichetti, M., Drysdale, R.N., Zanchetta, G., 2011. Hypogean microclimatology and hydrology of the 800–900 m a.s.l. level in the Monte Corchia Cave (Tuscany, Italy): Preliminary considerations and implications for paleoclimatological studies. Acta Carsologica 40, 175–187.

Bard, E., Delaygue, G., Rostek, F., Antonioli, F., Silenzi, S., Schrag, D.P., 2002. Hydrological conditions over the western Mediterranean basin during the deposition of the cold Sapropel 6 (ca. 175 kyr BP. Earth and Planetary Science Letters 202, 481–494.

Bar-Matthews, M., Ayalon, A., Kaufman, A., Wasserburg, G.J., 1999. The Eastern Mediterranean paleoclimate as a reflection of regional events: Soreq Cave, Israel. Earth and Planetary Science Letters 166, 85–95.

Bar-Matthews, M., Ayalon, A., Kaufmann, A., 2000. Timing and hydrological conditions of sapropel events in the eastern Mediterranean, as evident from speleothems, Soreq Cave, Israel. Chemical Geology 169, 145–156.

Bar-Matthews, M., Ayalon, A., Gilmour, M., 2003. Sea–land oxygen isotopic relationships from planktonic foraminifera and speleothems in the Eastern Mediterranean region and their implication for paleorainfall during interglacial intervals. Geochimica et Cosmochimica Acta 67, 3181–3199.

Berger, A., Loutre, M.F., 1991. Insolation values for the climate of the last 10 million years. Quaternary Science Reviews 10, 297–317.

Berti, F., 2010. Studio geochimico ed isotopico di suoli delle Alpi Apuane: Implicazioni per le ricostruzioni climatiche e paleoclimatiche. Master Thesis on Natural Sciences University of Pisa, pp. 1–115.

Bond, G., Kromer, B., Beer, J., Muscheler, R., Evans, M.N., Showers, W., Hoffman, S., Lotti-Bond, R., Hajadas, I., Bonani, G., 2001. Persistent solar influence on North Atlantic climate during Holocene. Science 7, 2130–2136.

Brauer, A., Allen, J.R.M., Mingram, J., Dulski, P., Wulf, S., Huntley, B., 2007. Evidence for the last interglacial chronology and environmental change from Southern Europe. Proceedings of the National Academy of Sciences of the United States of America 104, 450–455.

Broecker, W., Henderson, G., 1998. The sequence of events surrounding Termination II and their implications for the cause of glacial–interglacial CO2 changes. Paleoceanography 13, 352–364.

Cerling, T.E., Solomon, D.K., Quade, J., Bowman, J.R., 1991. On the isotopic composition of carbon in soil carbon dioxide. Geochimica et Cosmochimica Acta 55, 3404–3405.

Cheddadi, R., Rossignol-Strick, M., 1995. Eastern Mediterranean Quaternary paleoclimates from pollen and isotope records of marine cores in the Nile cone area. Paleoceanography 10, 291–300.

Cortecci, G., Dinelli, E., Indrizzi, M.C., Susini, C., Adorni-Braccesi, A., 1999. The Apuane Alps metamorphic complex, northern Tuscany: chemical and isotopic features of Grezzoni and Marmi Dolomitici. Atti Soc. Tosc. Sci. Nat. Mem. A 106, 79–89.

Couchoud, I., Genty, D., Hoffmann, D., Drysdale, R.N., Blamart, D., 2009. Millennial-scale variability during the Last Interglacial recorded in a speleothem from south-western France. Quaternary Science Reviews 28, 3263–3274.

Dansgaard, W., 1964. Stable isotopes in precipitation. Tellus 16, 436–468.

Day, C.C., Henderson, G.M., 2011. Oxygen isotopes in calcite under cave-analogue conditions. Geochimica et Cosmochimica Acta 75, 3956–3972.

Dorale, A., Liu, Z., 2005. Limitations of Hendy test criteria in judging the paleoclimatic suitability of speleothems and the need for replication. Journal of Cave and Karst Studies 71, 73–80.

Drysdale, R.N., Zanchetta, G., Hellstrom, J.C., Fallick, A.E., Zhao, J.X., Isola, I., Bruschi, G., 2004. Palaeoclimatic implications of the growth history and stable isotope ($\delta^{18}O$ and $\delta^{13}C$) geochemistry of a Middle to Late Pleistocene stalagmite from central-western Italy. Earth and Planetary Science Letters 227, 215–229.

Drysdale, R.N., Zanchetta, G., Hellstrom, J.C., Fallick, A.E., Zhao, J.X., 2005. Stalagmite evidence for the onset of the Last Interglacial in southern Europe at 129+/−1 ka. Geophysical Research Letters 32, 1–4.

Drysdale, R.N., Zanchetta, G., Hellstrom, J.C., Maas, R., Fallick, A.E., Pickett, M., Cartwright, I., Piccini, L., 2006. Late Holocene drought responsible for the collapse of Old World civilizations is recorded in an Italian cave flowstone. Geology 34, 101–104.

Drysdale, R.N., Zanchetta, G., Hellstrom, J.C., Fallick, A.E., McDonald, J., Cartwright, I., 2007. Stalagmite evidence for the precise timing of North Atlantic cold events during the early last glacial. Geology 35, 77–80.

Drysdale, R.N., Zanchetta, G., Hellstrom, J.C., Fallick, A.E., Sanchez-Goni, M.F., Couchoud, I., McDonald, J., Maas, R., Lohmann, G., Isola, I., 2009. Evidence for obliquity forcing of glacial termination II. Science 325, 1527–1531.

Dulinski, M., Rozanski, K., 1990. Formation of C-13 C-12 isotope ratios in speleothems—A semidynamic model. Radiocarbon 32, 7–16.

Fairchild, I.J., Baker, A., 2012. Speleothem science—From processes to past environments. Quaternary geosciences seriesWiley-Blakwell, pp. 3–370.

Fairchild, I.J., Smith, C.L., Baker, A., Fuller, L., Spötl, C., Mattey, D., McDermott, F., 2006. Modification and preservation of environmental signals in speleothems. Earth-Science Reviews 75 (1), 105–153.

Fletcher, W.J., Debret, M., Sanchez-Goni, M.F., 2012. Mid-Holocene emergence of a low frequency millennial oscillation in western Mediterranean climate: Implications for past dynamics of the North Atlantic atmospheric westerlies. The Holocene 1–14.

Follieri, M., Magri, D., Sadori, L., 1988. 250,000-year pollen record from Valle di Castiglione (Roma). Pollen et Spores 30, 329–356.

Frisia, S., Borsato, A., Fairchild, I.J., McDermott, F., 2000. Calcite fabrics, growth mechanisms and environments of formation in speleothems from the Italian Alps and southwestern Ireland. Journal of Sedimentary Petrology 70, 1183–1196.

Genty, D., Blamart, D., Ouahdi, R., Gilmour, M., Baker, A., Jouzel, J., Van-Exter, S., 2001. Precise dating of Dansgaard–Oeschger climate oscillations in western Europe from stalagmite data. Nature 421, 833–837.

Genty, D., Blamart, D., Ouahdi, R., Gilmour, M., Baker, A., Jouzel, J., Van-Exter, S., 2003. Precise dating of Dansgaard-Oeschger climate oscillations in western Europe from stalagmite data. Nature 421 (6925), 833–837.

Hellstrom, J.C., 2003. Rapid and accurate U/Th dating using parallel ion-counting multicollector ICP-MS. Journal of Analytical Atomic Spectrometry 18, 1346–1351.

Hellstrom, J.C., 2006. U-Th dating of speleothems with high initial 230Th using stratigraphical constraint. Quaternary Geochronology 1, 289–295.

Hendy, C.H., 1971. The calculation of the effects of different modes of formation on the isotopic composition of speleothems and their applicability as palaeoclimatic indicators. Geochimica et Cosmochimica Acta 35, 801–824.

Heusser, L., Oppo, D., 2003. Millennial- and orbital-scale climate variability in southeastern United States and in the subtropical Atlantic during Marine Isotope Stage 5: Evidence from pollen and isotopes in ODP Site 1059. Earth and Planetary Science Letters 214, 483–490.

Imbrie, J., Hays, J.D., Martinson, D.G., McIntyre, A., Mix, A.C., Morley, J.J., Pisias, N.G., Prell, W.L., 1984. The orbital theory of Pleistocene climate: Support from a revised chronology of the marine δ^{18} O record. Milankovitch and climate: Understanding the response to astronomical forcing, Proceedings of the NATO Advanced Research Workshop, p. 269.

Kallel, N., Duplessy, J.C., Labeyrie, L., Fontugne, M., Paterne, M., Montacer, M., 2000. Mediterranean pluvial periods and sapropel formation over the last 200 000 years. Palaeogeography, Palaeoclimatology, Palaeoecology 157 (1), 45–58.

Kim, S.T., O'Neill, J.R., 1997. Equilibrium and non-equilibrium oxygen isotope effects in synthetic carbonates. Geochimica et Cosmochimica Acta 61, 3461–3475.

Kolodny, Y., Stein, M., Machlus, M., 2005. Sea–rain–lake relation in the Last Glacial East Mediterranean revealed by $\delta^{18}O$-$\delta^{13}C$ in Lake Lisan aragonites. Geochimica et Cosmochimica Acta 69, 4045–4060.

Kukla, G., Mcmanus, J.F., Rousseau, D.D., Chuine, I., 1997. How long and how stable was the Last Interglacial? Quaternary Science Reviews 16, 605–612.

Kukla, G.J., Bender, M.L., de Beaulieu, J.L., Bond, G., W.S., Cleveringa, P., Gavin, J.E., Herbert, T.D., Imbrie, J., Jouzel, J., L.D., Knudsen, K.L., McManus, J.F., Merkt, J., Muhs, D.R., Muller, H., Poore, R.Z., Porter, S.C., Seret, G., Shackleton, N.J., Turner, C., Tzedakis, P.C., Winograd, I.J., 2002. Last interglacial climates. Quaternary Research 58, 2–13.

Lezine, A.M., Von Grafenstein, U., Andersen, N., Belmecheri, S., Bordon, A., Caron, B., Cazet, J.P., Erlenkeuser, H., Fouached, E., Grenier, C., Huntsman-Mapila, P., Hureau-Mazaudier, D., Manelli, D., Mazaud, A., Robert, C., Sulpizio, R., Tiercelin, J.J., Zanchetta, G., Zeqollari, Z., 2010. Lake Ohrid, Albania, provides an exceptional multi-proxy record of environmental changes during the last glacial–interglacial cycle. 287, 116–127.

Martrat, B., Grimalt, J.O., Lopez-Martinez, C., Chaco, I., Sierro, F.J., Flores, J.A., Zahn, R., Canals, M., Jason, H.C., Hodell, D.A., 2004. Abrupt temperature changes in the Western Mediterranean over the past 250,000 years. Science 306, 1762–1765.

Martrat, B., Grimalt, J.O., Shackleton, N.J., Deabreu, L., Hutterly, M.A., Stocker, T.F., 2007. Four climate cycles of recurring deep and surface water destabilizations on the Iberian Margin. Science 317 (5837), 502–507.

McDermott, F., Schwarcz, H., Rowe, J.P., 2006. In: Leng, M.J. (Ed.), Isotopes in speleothemes. Isotopes in paleoenvironmental research, vol 10, pp. 185–218.

McManus, J.F., Bond, G.C., Broecker, W.S., Johnsen, S., Labeyrie, L., Higgins, S., 1994. High-resolution climate records from the North Atlantic during the last interglacial. Nature 371, 326–329.

McManus, J.F., Oppo, D.W., Cullen, J.L., 1999. A 0.5-million-year record of millennial-scale climate variability in the North Atlantic. Science 283, 971–975.

McManus, J.F., Oppo, D.W., Keigwin, L.D., Cullen, J.L., Bond, G.C., 2002. Thermohaline circulation and prolonged interglacial warmth in the North Atlantic. Quaternary Research 58, 17–21.

https://doi.org/10.1016/j.yqres.2014.05.005 Published online by Cambridge University Press

Méliéres, M.A., Rossignol-Strick, M., Malaize, B., 1997. Relation between low latitude insolation and $\delta^{18}O$ change of atmospheric oxygen for the last 200 kyrs, as revealed by Mediterranean sapropels. Geophysical Research Letters 24, 1235–1238.
Mickler, P.J., Stern, L.A., Banner, J.L., 2006. Large kinetic isotope effects in modern speleothems. GSA Bulletin 118, 65–81.
Mühlinghaus, C., Scholz, D., Mangini, A., 2009. Modelling fractionation of stable isotopes in stalagmites. Geochimica et Cosmochimica Acta 73, 7275–7289.
Mussi, M., Leone, G., Nardi, I., 1998. Isotopic composition of natural waters from the Alpi Apuane-Garfagnana area, northern Tuscany, Italy. Mineralogica Petrographica Acta 41, 163–178.
Oppo, D.W., Keigwin, L.D., McManus, J.F., 2001. Persistent suborbital climate variability in marine isotope stage 5 and Termination II. Paleoceanography 16, 280–292.
Oppo, D.W., McManus, J.F., Cullen, J.L., 2006. Evolution and demise of the Last Interglacial warmth in the subpolar North Atlantic. Quaternary Science Reviews 25, 3268–3277.
Oster, J.L., Montanez, I.P., Guilderson, T.P., Sharp, W.D., Banner, J.L., 2010. Modeling speleothem $\delta^{13}C$ variability in a central Sierra Nevada cave using ^{14}C and $^{87}Sr/^{86}Sr$. Geochimica et Cosmochimica Acta 74, 5228–5242.
Pandeli, E., Bagnoli, P., Negri, M., 2004. The Fornovolasco schists of the Apuan Alps (Northern Tuscany, Italy): A new hypothesis for their stratigraphic setting. Bollettino Società Geologica 123, 53–66.
Piccini, L., Pranzini, G., Tedici, L., Forti, P., 1999. Le risorse idriche dei complessi carbonatici del comprensorio apuo-versiliese. Quaderni di Geologia Applicata 6, 61–78.
Piccini, L., Zanchetta, G., Drysdale, R.N., Hellstrom, J.C., Isola, I., Fallick, A.E., Leone, G., Doveri, M., Mussi, M., Mantelli, F., Molli, G., Lotti, L., Roncioni, A., Regattieri, E., Meccheri, M., Vaselli, L., 2008. The environmental features of the Monte Corchia cave system (Apuan Alps, central Italy) and their effects on speleothem growth. International Journal of Speleology 37, 153–172.
Rasmussen, T.L., Thomsen, E., Kuijpers, A., Wastegård, S., 2003. Late warming and early cooling of the sea surface in the Nordic seas during MIS 5e (Eemian Interglacial). Quaternary Science Reviews 22, 809–821.
Regattieri, E., Isola, I., Zanchetta, G., Drysdale, R.N., Hellstrom, J.C., Baneschi, I., 2012. Stratigraphy, petrography and chronology of speleothem deposition at Tana che Urla (Lucca, Italy): Paleoclimatic implications. Geografia Fisica e Dinamica del Quaternario 35, 141–152.
Regattieri, E., Zanchetta, G., Drysdale, R.N., Isola, I., Hellstrom, J.C., Dallai, L., 2014. Late-glacial to Holocene trace element record (Ba, Mg, Sr) from Corchia Cave (Apuan Alps, central Italy): Paleoenvironmental implications. Journal of Quaternary Science 29, 381–392.
Richards, D.A., Dorale, J.A., 2003. Uranium-series chronology and environmental applications of speleothems. Reviews in Mineralogy and Geochemistry 52, 407–460.
Romanek, C.S., Grossman, E.L., Morse, J.W., 1992. Carbon isotopic fractionation in synthetic aragonite and calcite: Effects of temperature and precipitation rate. Geochimica et Cosmochimica Acta 56, 419–430.
Rossignol-Strick, M., 1983. African monsoons, as immediate climate response to orbital insolation. Nature 304, 46–48.
Rossignol-Strick, M., 1985. Mediterranean Quaternary sapropels, an immediate response of the African monsoon to variation of insolation. Palaeogeography, Palaeoclimatology, Palaeoecology 49, 237–263.
Rudzka, D., McDemott, F., Baldini, L.M., Fleitmann, D., Moreno, A., Stoll, H., 2011. The coupled $\delta^{13}C$-radiocarbon systematics of three Late Glacial/early Holocene speleothems; insights into soil and cave processes at climatic transitions. Geochimica et Cosmochimica Acta 75, 4321–4339.
Sánchez Gõni, M.E., Turon, J.-L., Eynaud, F., Shackleton, N.J., 1999. High resolution palynological record off the Iberian margin: Direct land–sea correlation for the Last Interglacial complex. Earth and Planetary Science Letters 171, 123–137.
Sanchez-Goni, M.F., 2005. Introduction to climate and vegetation in Europe during MIS5. The climate of the past interglacial. Developments in quaternary science, 7, pp. 197–205.
Scholz, D., Hoffmann, D.L., Hellstrom, J., Bronk Ramsey, C., 2012. A comparison of different methods for speleothem age modelling. Quaternary Geochronology 14, 94–104.
Sprovieri, R., Di Stefano, E., Incarbona, A., Oppo, D.W., 2006. Suborbital climate variability during Marine Isotopic Stage 5 in the central Mediterranean basin: Evidence from calcareous plankton record. Quaternary Science Reviews 25, 2332–2342.
Tremaine, D.M., Froelich, P.N., Wang, Y., 2011. Speleothem calcite farmed in situ: Modern calibration of $\delta^{18}O$ and $\delta^{13}C$ paleoclimate proxies in a continuously-monitored natural cave system. Geochimica et Cosmochimica Acta 75, 4929–4950.
Tzedakis, P.C., Raynaud, D., McManus, J.F., Berger, A., Brovkin, V., Kiefer, T., 2009. Interglacial diversity. Nature Geoscience 2, 751–755.
Vergnaud-Grazzini, C., Ryan, W.B.F., Cita, M.B., 1977. Stable isotope fractionation, climate change and episodic stagnation in the Eastern Mediterranean during the late Quaternary. Marine Micropaleontology 2, 353–370.
Vogel, H., Zanchetta, G., Sulpizio, R., Wagner, B., Nowaczyk, N., 2009. A tephrostratigraphic record for the last glacial–interglacial cycle from Lake Ohrid, Albania and Macedonia. Journal of Quaternary Science 25, 320–338.
Wainer, K., Genty, D., Daeron, M., Bar-Matthews, M., Vonhof, H., Dublyansky, Y., Pons-Branchu, E., Thoma, L., van Calsteren, P., Quiunif, Y., Caillon, N., 2011. Speleothem record of the last 180 ka in Villars cave (SW France): Investigation of a large $\delta^{18}O$ shift between MIS6 and MIS5. Quaternary Science Reviews 30, 130–146.
Zanchetta, G., Drysdale, R.N., Hellstrom, J.C., Fallick, A.E., Isola, I., Gagan, M., Pareschi, M.T., 2007. Enhanced rainfall in the western Mediterranean during deposition of sapropel S1: Stalagmite evidence from Corchia Cave (Central Italy). Quaternary Science Reviews 26, 279–286.
Zhang, J., Quay, P.D., Wilbur, D.O., 1995. Carbon isotope fractionation during gas-water exchange and dissolution of CO_2. Geochimica et Cosmochimica Acta 59, 107–114.
Zhornyak, L.V., Zanchetta, G., Drysdale, R.N., Hellstrom, J.C., Isola, I., Regattieri, E., Piccini, L., Baneschi, I., Couchoud, I., 2011. Stratigraphic evidence for a "pluvial phase" between ca 8200 and 7100 ka from Renella cave (Central Italy). Quaternary Science Reviews 30, 409–417.

https://doi.org/10.1016/j.yqres.2014.05.005 Published online by Cambridge University Press